

# Apoptosis in Transgenic Mice Expressing the P301L Mutated Form of Human Tau

Rita M Ramalho,<sup>1</sup> Ricardo J S Viana,<sup>1</sup> Rui E Castro,<sup>1</sup> Clifford J Steer,<sup>2</sup> Walter C Low,<sup>3,4</sup> and Cecília M P Rodrigues<sup>1</sup>

<sup>1</sup>iMed.UL, Faculty of Pharmacy, University of Lisbon, Av. Prof. Gama Pinto, Lisbon, Portugal; <sup>2</sup>Departments of Medicine, and Genetics, Cell Biology, and Development, University of Minnesota Medical School, Minneapolis, Minnesota; <sup>3</sup>Department of Neurosurgery, University of Minnesota Medical School, Minneapolis, Minnesota; <sup>4</sup>Graduate Program in Neuroscience, University of Minnesota Medical School, Minneapolis, Minnesota, United States of America

The rTg4510 mouse is a tauopathy model, characterized by massive neurodegeneration in Alzheimer's disease (AD)-relevant cortical and limbic structures, deficits in spatial reference memory, and progression of neurofibrillary tangles (NFT). In this study, we examined the role of apoptosis in neuronal loss and associated tau pathology. The results showed that DNA fragmentation and caspase-3 activation are common in the hippocampus and frontal cortex of young rTg4510 mice. These changes were associated with cleavage of tau into smaller intermediate fragments, which persist with age. Interestingly, active caspase-3 was often co-localized with cleaved tau. *In vitro*, fibrillar A $\beta_{1-42}$  resulted in nuclear fragmentation, caspase activation, and caspase-3-induced cleavage of tau. Notably, incubation with the antiapoptotic molecule tauroursodeoxycholic acid abrogated apoptosis-mediated cleavage of tau in rat cortical neurons. In conclusion, caspase-3-cleaved intermediate tau species occurred early in rTg4510 brains and preceded cell loss in A $\beta$ -exposed cultured neurons. These results suggest a potential role of apoptosis in neurodegeneration.

Online address: <http://www.molmed.org>  
doi: 10.2119/2007-00133.Ramalho

## INTRODUCTION

Alzheimer's disease (AD) is a progressive neurodegenerative disease with extracellular plaques of amyloid  $\beta$  (A $\beta$ ) and intracellular aggregations of tau (1). In AD and other tauopathies, tau loses its capacity to bind microtubules, migrates to the cell body, and aggregates into neurofibrillary tangles (NFT) (2). Post-translational conformational changes of tau, such as abnormal hyperphosphorylation and proteolysis increase its ability to aggregate (3,4).

The role of apoptosis in AD and other tauopathies is still controversial. Nevertheless, apoptosis is increased (5) and caspase-3 activated (6) in AD brains. Interestingly, tau can be cleaved by caspase-3 at Asp421 in its C-terminal re-

gion, resulting in an N-terminal product detected in cultured neurons, in AD brains (7), and in other tauopathies (8). Truncated tau plays a role in nucleation-dependent filament formation of tau and induces neuronal death. Moreover, caspase-3-cleaved tau often colocalizes with A $\beta$  peptide deposition, suggesting a link between amyloid plaques and NFT formation (9).

The rTg4510 mouse model is a robust model of tauopathy, with massive neurodegeneration in specific cortical and limbic structures, leading to forebrain atrophy and brain weight loss (10–12). In addition, the progression of NFT pathology and neuronal loss is correlated with early deficits in spatial reference memory. The suppression of trans-

gene expression prevents further loss of neurons and enables partial recovery of cognitive functions, but does not inhibit the progression of NFT. This suggests that NFT formation is not directly responsible for neurodegeneration and memory loss in rTg4510. Instead, toxic intermediate tau species may trigger further neurodegeneration.

Ursodeoxycholic acid (UDCA) and tauroursodeoxycholic acid (TUDCA) are endogenous bile acids that increase the apoptotic threshold in several cell types (13,14). We have shown previously that TUDCA stabilizes mitochondrial function and prevents A $\beta$ -induced apoptosis (15–17). Furthermore, TUDCA was neuroprotective in a transgenic mouse model of Huntington's disease (18), reduced lesion volumes in rat models of stroke (19,20), improved the survival and function of nigral transplants in a rat model of Parkinson's disease (21), and partially rescued a Parkinson's disease model of *Caenorhabditis elegans* from mitochondrial dysfunction (22).

---

**Address correspondence and reprint requests to** Cecília M P Rodrigues, iMed.UL, Faculty of Pharmacy, University of Lisbon, Av. Prof. Gama Pinto, 1649-003, Lisbon, Portugal; Phone: +351 21 794 6400; Fax: +351 21 794 6491; E-mail: [cmprodrigues@ff.ul.pt](mailto:cmprodrigues@ff.ul.pt).  
Submitted December 17, 2007; Accepted for publication March 17, 2008; Epub ([www.molmed.org](http://www.molmed.org)) ahead of print March 27, 2008.

Using rTg4510 mice, we investigated the role of apoptosis in neuronal loss and tau-associated pathology. Our results suggest that apoptosis is an early event associated with tau cleavage in the hippocampus and the frontal cortex. Cleaved tau, in turn, appears to represent a toxic form of tau. In cultured cortical neurons, apoptosis and caspase-3 cleavage of tau induced by fibrillar  $A\beta_{1-42}$  were inhibited significantly by TUDCA. Thus, caspase-3-cleaved intermediate tau species may be responsible, in part, for toxicity in rTg4510 brains and cell loss in  $A\beta$ -exposed cultured neurons. These results suggest a role of apoptosis in neurodegeneration.

## MATERIALS AND METHODS

### Generation of Transgenic Mice

The rTg4510 is a recently developed mouse model of tauopathy in which expression of human tau, containing the frontotemporal dementia-associated P301L mutation, can be suppressed with doxycycline administration (10). Briefly, the method for generating rTg4510 mice utilized a system of responder and activator transgenes. Mice expressing the activator transgene, consisting of a four-repeat human tau with the P301L mutation placed downstream of a tetracycline operon responsive element were successively backcrossed at least five times onto a 129S6 background strain. Responder mice, consisting of a tet-off open reading frame placed downstream of  $Ca^{2+}$ -*calmodulin kinase II* promoter elements were maintained in the FVB/N strain. From this, double transgenic mice were generated in which expression of the P301L tau expression was restricted to the forebrain structures. Mice were screened by PCR using the primer pairs 5'-GAT TAA CAG CGC ATT AGA GCT G-3' and 5'-GCA TAT GAT CAA TTC AAG GCC GAT AAG-3' for activator transgenes, and 5'-TGA ACC AGG ATG GCT GAG CC-3' and 5'-TTG TCA TCG CTT CCA GTC CCC G-3' for responder transgenes. Tau-expressing mice and littermate control mice (lacking either the tau responder

transgene or the activator transgene) between 2.5 and 8.5 months were used (four to ten animals in each group, per age). Animals were killed with an overdose of ketamine xylazine cocktail via an intraperitoneal cavity injection. The chest cavity then was opened by cutting through the diaphragm and rib cage laterally. The right atrium was cut to drain blood; and the left ventricle punctured for cannula placement. PBS was flushed through the circulatory system using a pressure of 60 mmHg for 3 to 4 min or until the right atrium was cleared. The brain was removed and rapidly frozen in dry ice. Cryostat brain sections of 10  $\mu$ m were prepared for analysis of transgenic and control mice. In addition, different areas of the brain were isolated, including the olfactory bulb, frontal cortex, sensorimotor cortex, medial septal nucleus, hippocampus, and entorhinal cortex. All brain areas were limited, sliced using a cryostat, and separated from other structures by laboratory personnel with knowledge in mice brain anatomy.

All animals were housed and tested according to standards established by the American Association for the Accreditation of Laboratory Animal Care and Institutional Animal Care and Use Committee guidelines, with every effort made to minimize the number of animals used.

### Isolation and Culture of Rat Cortical Neurons

Primary cultures of rat cortical neurons were prepared from 17- to 18-day-old fetuses of Wistar rats as described previously (23) with minor modifications. In short, pregnant rats were ether-anesthetized and decapitated. The fetuses were collected in Hank's balanced salt solution (HBSS-1; Invitrogen, Grand Island, NY, USA) and rapidly decapitated. After removal of meninges and white matter, the brain cortex was collected in Hank's balanced salt solution without  $Ca^{2+}$  and  $Mg^{2+}$  (HBSS-2). The cortex was then mechanically fragmented, transferred to a 0.025% trypsin in HBSS-2 solution, and incubated for 15 min at 37° C. Following trypsinization, cells were washed twice in

HBSS-2 containing 10% fetal calf serum (FBS) and re-suspended in Neurobasal medium (Invitrogen), supplemented with 0.5 mM L-glutamine, 25  $\mu$ M L-glutamic acid, 2% B-27 supplement (Invitrogen), and 12 mg/mL gentamicin. Neurons then were plated on tissue culture plates, precoated with poly-D-lysine at  $1 \times 10^6$  cells/mL, and maintained at 37° C in a humidified atmosphere of 5%  $CO_2$ . All experiments were performed on cells cultured for 4 d in fresh medium without glutamic acid and B-27 supplement. Cells were characterized by phase contrast microscopy and indirect immunocytochemistry for neurofilaments and glial fibrillary acidic protein. Neuronal cultures were > 95% pure. After 4 d in culture, isolated rat neurons were incubated with 20  $\mu$ M  $A\beta_{1-42}$  (Bachem AG, Budendorf, Switzerland) that had been induced to form fibrils by preincubation in culture medium, as described previously (9). In short, 0.45 mg of  $A\beta_{1-42}$  peptide was dissolved in 20  $\mu$ L of DMSO and diluted to a 100  $\mu$ M stock solution in medium, which then was incubated with gentle shaking at room temperature for 4 d. Fibrillar  $A\beta_{1-42}$  then was diluted to 20  $\mu$ M and applied to neuron cultures; 0.2% DMSO was added to control cultures. Cortical neurons were incubated with fibrillar  $A\beta_{1-42}$  for 24 h, with or without 100  $\mu$ M TUDCA (Sigma Chemical, St. Louis, MO, USA), or no addition. In co-incubation experiments, TUDCA was added to neurons 12 h prior to incubation with  $A\beta_{1-42}$ . In a subset of experiments, cells were incubated with 50  $\mu$ M z-VAD.fmk (Sigma Chemical), a general caspase inhibitor, for 1 h prior to  $A\beta_{1-42}$  incubation.

### Evaluation of Apoptosis and Caspase-3 Activation

DNA fragmentation in brain sections of both transgenic and control mice was detected using an ApopTag peroxidase *in situ* apoptosis detection kit (Serologicals Corp, Norcross, GA, USA) for transferase mediated dUTP-digoxigenin nick-end labeling (TUNEL) staining. In brief, tissue sections were fixed in 4% paraformaldehyde in PBS, pH 7.4, for 10 min at room

temperature, post-fixed in precooled ethanol:acetic acid (2:1, v/v) for 5 min at  $-20^{\circ}\text{C}$ , and treated with 3% hydrogen peroxide to quench endogenous peroxidase activity. After adding the equilibration buffer, sections were treated with terminal deoxynucleotidyltransferase (TdT) and digoxigenin-dNTPs for 60 min at  $37^{\circ}\text{C}$ . Specimens were then treated with anti-digoxigenin-peroxidase for 30 min at  $37^{\circ}\text{C}$ , colorized with 3,3'-diaminobenzidine (DAB) substrate, and counterstained with 0.5% methyl green. Finally, slides were rinsed, dehydrated, and mounted. A negative control was prepared by omitting the TdT enzyme to control for non-specific incorporation of nucleotides or binding of enzyme-conjugate. The specimens were examined using a bright-field microscope (Zeiss Axioskop; Carl Zeiss GmbH, Jena, Germany) and the data expressed as the number of TUNEL-positive cells/high-power field ( $\times 400$ ) in at least five high-power fields.

Cell viability of cortical neurons was assessed using trypan blue dye exclusion and confirmed by lactate dehydrogenase viability assays (Sigma-Aldrich). In addition, Hoechst labeling of cells was used to detect apoptotic nuclei. Briefly, the medium was gently removed to prevent detachment of cells. Attached neurons were fixed with 4% paraformaldehyde in phosphate-buffered saline (PBS), pH 7.4, for 10 min at room temperature, incubated with Hoechst dye 33258 (Sigma-Aldrich) at  $5\ \mu\text{g}/\text{mL}$  in PBS for 5 min, washed with PBS, and mounted using PBS:glycerol (3:1, v/v). Fluorescent nuclei were scored blindly and categorized according to the condensation and staining characteristics of chromatin. Normal nuclei showed non-condensed chromatin dispersed over the entire nucleus. Apoptotic nuclei were identified by condensed chromatin, contiguous to the nuclear membrane, as well as nuclear fragmentation of condensed chromatin. Three random microscopic fields per sample of  $\sim 250$  nuclei were counted and mean values expressed as the percentage of apoptotic nuclei.

Finally, caspase activation was determined in cytosolic protein extracts from

brain tissue and cell cultures. Samples were homogenized in isolation buffer, containing 10 mM Tris-HCl buffer, pH 7.6, 5 mM  $\text{MgCl}_2$ , 1.5 mM KAc, 2 mM DTT, and protease inhibitor cocktail tablets (Complete; Roche Applied Science, Mannheim, Germany). General caspase-3-like activity was determined by enzymatic cleavage of chromophore *p*-nitroanilide (pNA) from the substrate *N*-acetyl-Asp-Glu-Val-Asp-pNA (DEVD-pNA; Sigma Chemical). The proteolytic reaction was carried out in isolation buffer containing 50  $\mu\text{g}$  cytosolic protein and 50  $\mu\text{M}$  DEVD-pNA. The reaction mixtures were incubated at  $37^{\circ}\text{C}$  for 1 h, and the formation of pNA was measured at 405 nm using a 96-well plate reader.

### Immunoblotting

Levels of caspase-3-cleaved tau protein were determined by Western blot analysis. Briefly, 50  $\mu\text{g}$  of total protein extracts were separated on 12% SDS-polyacrylamide electrophoresis minigels. Following electrophoretic transfer onto nitrocellulose membranes, immunoblots were incubated with 15%  $\text{H}_2\text{O}_2$  for 15 min at room temperature. After blocking with 5% nonfat milk solution, the blots were incubated overnight at  $4^{\circ}\text{C}$  with primary mouse monoclonal antibodies reactive to caspase-cleaved tau (truncated at Asp421) (MAB5430; Chemicon, Billerica, MA, USA) and, finally, with a secondary antibody conjugated with horseradish peroxidase (Bio-Rad Laboratories, Hercules, CA, USA) for 3 h at room temperature. The membranes were processed for protein detection using Super Signal substrate (Pierce, Rockford, IL, USA). Total tau (clone T14, Zymed Laboratories Inc, San Francisco, CA, USA) was used as a loading control. Protein concentrations were determined using the Bio-Rad protein assay kit according to the manufacturer's specifications.

### Immunohistochemistry

Light-level immunohistochemistry was performed in fixed brain sections to detect caspase-3-cleaved tau. Briefly, slides were soaked in 3% hydrogen peroxide, 10%

methanol for 10 min, washed, and incubated in serum blocking solution (Santa Cruz Biotechnology, Santa Cruz, CA, USA) with 0.3% Triton X-100 for 1 h. Specimens then were incubated with primary antibody overnight at  $4^{\circ}\text{C}$ . After rinsing, specimens were incubated with biotinylated secondary antibody and a horseradish peroxidase-streptavidin complex, for 1 h each. Tissue samples then were colorized with DAB substrate, counterstained, mounted, and visualized in a bright-field microscope (Zeiss Axioscope).

Immunofluorescence was performed to investigate the co-localization of caspase-cleaved tau (truncated at Asp421) and active caspase-3 in brain tissue and cultured cells. Fixed brain sections were soaked in 0.3% hydrogen peroxide for 5 min, washed, and blocked (0.3% Triton X-100, 10% donkey serum, 1% FBS) for 1 h. In addition, cortical neurons were washed with PBS, incubated for 30 s in microtubule stabilization buffer, and fixed for 10 min in 4% paraformaldehyde at room temperature. Fixed cultured cells were incubated with 1% nonfat milk in PBS containing 1% bovine serum albumin and 1.5% Triton X-100 for 1 h at room temperature. Specimens then were incubated with both monoclonal caspase-cleaved tau and polyclonal caspase-3 (Santa Cruz Biotechnology) antibodies overnight at  $4^{\circ}\text{C}$ . After rinsing, specimens then were incubated with either fluorescently labeled anti-mouse or anti-rabbit (CyTM2 and CyTM5, respectively; Jackson ImmunoResearch Laboratories, Inc, West Grove, PA, USA) for 2 h at room temperature. Adequate controls were prepared by omitting the primary antibody or using preimmune IgG, which eliminated all labeling. Samples then were mounted and visualized in a MRC1000 confocal microscope (Bio-Rad, Hercules, CA, USA). Finally, the percentage of caspase-cleaved tau and active caspase-3-positive cortical neurons with apoptotic nuclei was determined by staining with Hoechst 33258.

### Densitometry and Statistical Analysis

The relative intensities of protein bands were analyzed using the Image-

Master 1D Elite v4.00 densitometric analysis program (Amersham Biosciences, Piscataway, NJ, USA). All data were expressed as mean  $\pm$  SEM from at least three separate experiments. Statistical analysis was performed using GraphPad InStat version 3.00 for Windows 95 (GraphPad Software, San Diego, CA, USA) for the Student *t* test. Values of *P* < 0.05 were considered significant.

**RESULTS**

**TUNEL-Positive Cells and Caspase Activation in the Frontal Cortex and Hippocampus of Young rTg4510 Animals**

AD is a progressive neurodegenerative disease with well-defined spatial and temporal lesions that correlate with neuronal loss. The entorhinal cortex and hippocampus are particularly vulnerable (24), while other cortical and subcortical areas are influenced as the disease progresses. Frontotemporal dementias affect mostly the frontal and temporal cortex, although with wide ranging pathology in subcortical and brainstem regions. Previous studies using rTg4510 mice showed marked brain atrophy with massive neuronal loss, especially in the hippocampus (10). The dentel gyrus showed the earliest onset of neuronal loss at 2.5 months of age (85% of total neuronal loss), followed by CA1 and CA2/3 regions at 5.5 months (69% to 82%), and cortex at 8.5 months (52%) (12). However, the role of apoptosis in neurodegeneration of rTg4510 mice remained unclear.

In this study, levels of apoptosis in brain slices of control and rTg4510 mice at 2.5, 5.5, and 8.5 months were evaluated using the TUNEL assay. At 2.5 months, transgenic animals showed significant levels of TUNEL-positive cells in specific regions of the brain, including the frontal cortex (FC) (*P* < 0.05), and the medial septal nucleus (MSN) (*P* < 0.01), subgranular zone (SGZ) (*P* < 0.01), and subventricular zone (SVZ) (*P* < 0.05) of the hippocampus (Figure 1A, upper histogram). Labeled cells showed morphologic features consistent with the pheno-

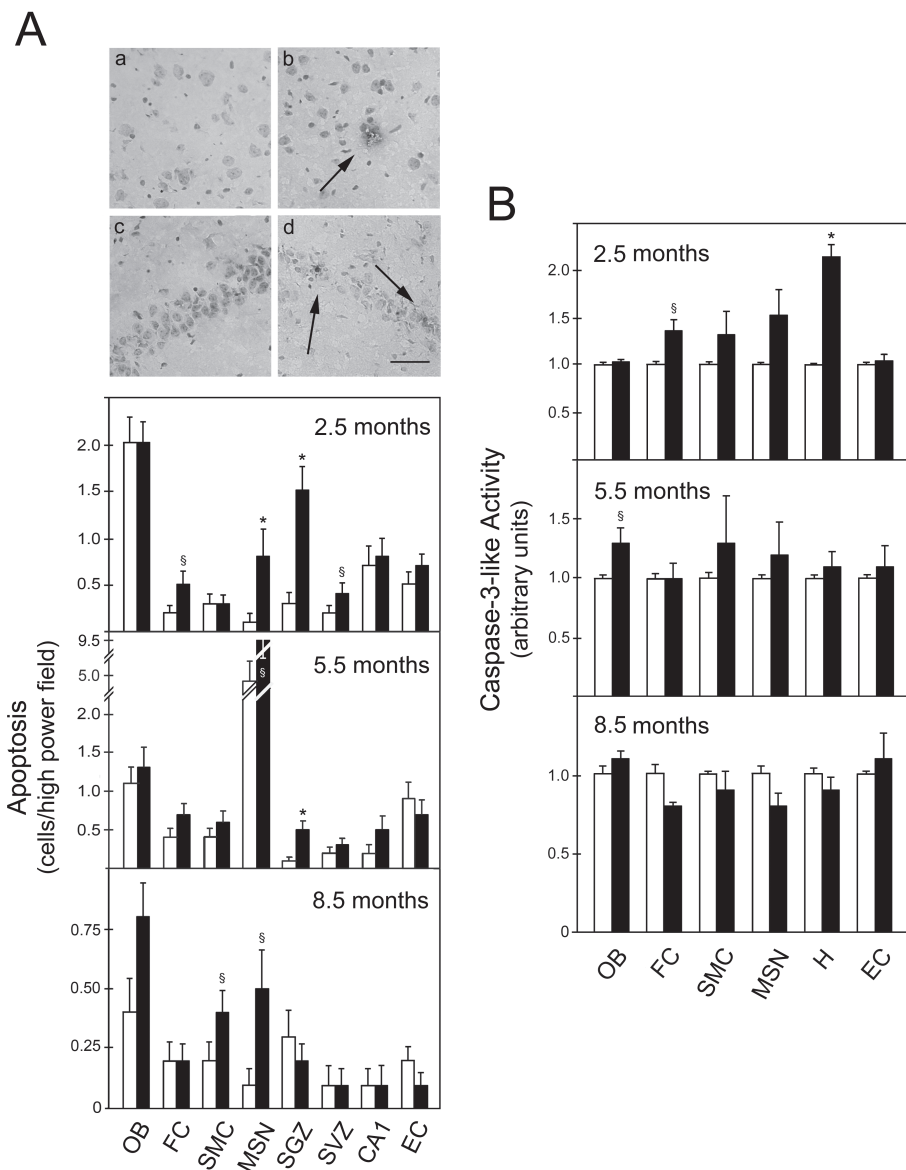


**Figure 1.** DNA fragmentation and caspase-3 activation occur early in the frontal cortex and hippocampus of rTg4510 mice. Brain slices were analyzed from both control (white bars) and transgenic animals (black bars) at 2.5, 5.5, and 8.5 months. DNA fragmentation was assessed by the TUNEL assay, and the number of positive cells was counted in the olfactory bulb (OB), frontal cortex (FC), sensorimotor cortex (SMC), medial septal nucleus (MSN), subgranular zone (SGZ), subventricular zone (SVZ), CA1, and entorhinal cortex (EC). Cytosolic proteins were extracted for caspase-3-like activity assays from OB, FC, SMC, MSN, hippocampus (H), and EC of both control and transgenic animals at 2.5, 5.5, and 8.5 months. A: TUNEL staining in control FC (a); transgenic FC (b); control H (c); and transgenic H (d) at 2.5 months (top) and number of apoptotic cells (bottom). Apoptotic nuclei were identified by a condensed nucleus with dark staining (arrows). B: DEVD-specific caspase activity. The results are expressed as mean  $\pm$  SEM of at least three different experiments. \**P* < 0.01 and §*P* < 0.05 from control animals. Scale bar: 100  $\mu$ m.

type of apoptosis, including nuclear condensation and fragmentation. In addition, rTg4510 animals at 5.5 months had increased apoptosis only in the MSN ( $P < 0.05$ ) and SGZ ( $P < 0.01$ ) (Figure 1A, middle histogram). Finally, the number of apoptotic cells in transgenic animals at 8.5 months was similar to controls, except in the sensorimotor cortex (SMC) and MSN ( $P < 0.05$ ) (Figure 1A, lower histogram).

As a hallmark of apoptosis, caspase-3 activation was investigated in both control and transgenic animals. Consistent with TUNEL data, caspase-3-like activity was increased in FC ( $P < 0.05$ ) and hippocampus ( $P < 0.01$ ) at 2.5 months (Figure 1B, upper histogram). At 5.5 months, despite the significant increase of TUNEL-positive cells, caspase-3 activity was altered only marginally in the hippocampus (Figure 1B, middle histogram). Finally, no significant changes were detected at 8.5 months (Figure 1B, lower histogram). Taken together, these findings indicate that DNA fragmentation and caspase-3 activation are early events in the frontal cortex and hippocampus of rTg4510, which may precede massive neuronal loss (10).

### Caspase-3 Activation is Associated with Tau Cleavage in rTg4510 Animals

Tau protein is functionally and structurally altered in AD and other tauopathies. In fact, posttranslational changes such as abnormal phosphorylation and cleavage result in altered solubility and conformation, as well as aggregation (3,4). Next, we focused our study in the frontal cortex and hippocampus of rTg4510, which showed increased apoptosis, and investigated patterns of tau expression with aging. Using the antibody T14 to detect total human tau, we detected small fragments of ~50 kDa and lower molecular weights, which were present only in animals at 2.5 months (data not shown). Cleaved fragments may represent pathological forms of tau and are associated with increased apoptosis. In fact, cleavage of tau at

Asp421 of the C-terminal region by caspase-3 has been detected both in neurons and AD brains (7).

To determine if caspase-3 was responsible for cleavage of tau, we performed immunohistochemistry assays using a specific antibody that only recognizes the Asp421-cleaved tau fragment. At 2.5 months, the number of caspase-cleaved tau cells was significantly higher in FC and SGZ ( $P < 0.01$ ) (Figure 2A). The number of positive cells also was significantly higher in the olfactory bulb ( $P < 0.01$ ), SMC ( $P < 0.05$ ), and entorhinal cortex ( $P < 0.01$ ) in transgenic animals. Consistently, Western blot analysis showed that caspase-cleaved tau was already detected at 2.5 months (Figure 2B). The ~50 kDa fragment also was evident in older animals, suggesting that tau persists during tangle maturation and neurodegeneration in older animals (7,10,12). Levels of caspase-cleaved tau decreased more in the frontal cortex than the hippocampus at 8.5 months. In fact, this may have resulted from greater removal of these cells from the cortex, which is in agreement with previous reports (12).

Results from control animals were consistent with those obtained by immunohistochemistry (data not shown). Finally, we performed co-immunohistochemistry analysis of brain slices to determine if cleaved tau co-localized with active caspase-3 in the frontal cortex and hippocampus. By confocal microscopy, labeled cleaved tau was readily detectable in transgenic animals (Figure 3). Active caspase-3, however, was less obvious, showing more of a diffuse pattern, and almost absent in control animals (data not shown). Nevertheless, cleaved tau was often co-localized with active caspase-3 in the frontal cortex and hippocampus of transgenic animals at 2.5 months. This suggests that active caspase-3 may be responsible for cleavage of tau in younger rTg4510 animals, specifically in the frontal cortex and hippocampus. Cleaved tau persists with age, possibly with a significant role in NFT formation.

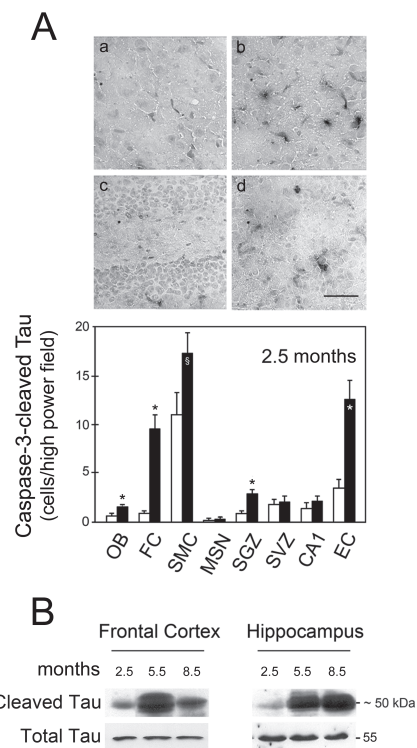


**Figure 2.** Tau cleavage is an early event modulated by caspase-3 activation in rTg4510 mice. Brain slices were analyzed from both control (white bars) and transgenic animals (black bars) at 2.5 months. Caspase-cleaved tau (truncated at Asp421) cells were identified by immunohistochemistry and the number of positive cells was counted in the olfactory bulb (OB), frontal cortex (FC), sensorimotor cortex (SMC), medial septal nucleus (MSN), subgranular zone (SGZ), subventricular zone (SVZ), CA1, and entorhinal cortex (EC). Total proteins of frontal cortex and hippocampus of both control and transgenic animals at 2.5, 5.5, and 8.5 months were extracted and analyzed by Western blot. A: Immunohistochemical staining in control FC (a); transgenic FC (b); control H (c); and transgenic H (d) (top) and number of caspase-cleaved tau positive cells (bottom). Positive cells were identified by dark staining. B: Representative immunoblots of caspase-cleaved tau. The results are expressed as mean  $\pm$  SEM of at least three different experiments. \* $P < 0.01$  and § $P < 0.05$  from control animals. The blots were normalized to total tau protein levels. Scale bar: 100  $\mu$ m.

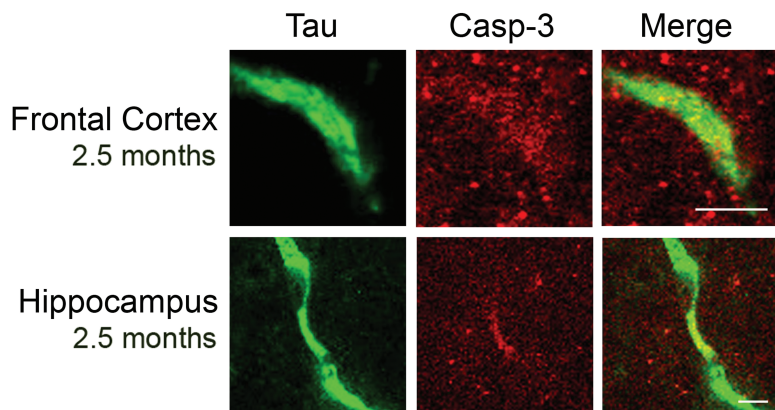


**Figure 3.** Active caspase-3 is co-localized with cleaved tau in the frontal cortex and hippocampus of transgenic animals at 2.5 months. Brain slices were analyzed from both control and transgenic animals at 2.5 months. Co-localization of active caspase-3 and caspase-cleaved tau was evaluated in the frontal cortex and hippocampus by fluorescent immunohistochemistry and confocal microscopy. Scale bar: 20  $\mu$ m.

**Modulation of A $\beta$ -Induced Toxicity and Cleavage of Tau in Cortical Neurons**

Amyloid plaques and NFT have been categorized largely as independent neuropathologic phenomena. In tauopathies, mutations in tau are thought to be sufficient to induce its aggregation in NFT and the consequent neuronal dysfunction, without the presence or aggregation of A $\beta$ . However, in AD, there are no described mutations in tau and studies have suggested that tau is necessary for A $\beta$ -induced cognitive dysfunction (25). In fact, only a direct or indirect interaction between A $\beta$  and tau could explain the mechanistic development of AD, although a correlation between the amyloid precursor protein (APP) and tau could not be ruled out. A possible link would be A $\beta$ -induced caspase-3 activation, followed by cleavage and subsequent aggregation of tau (9). Thus, we examined this correlation in primary rat cortical neurons incubated with fibrillar A $\beta_{1-42}$  and investigated the potential modulation by incubation with the antiapoptotic bile acid, TUDCA. General cell death increased after A $\beta_{1-42}$  incubation but not after scrambled A $\beta_{1-42}$  as evaluated by trypan blue dye exclusion and lactate dehydrogenase viability assays (data not shown). Nuclear fragmentation characteristic of apoptosis increased

to ~30% ( $P < 0.01$ ) in cells exposed to A $\beta_{1-42}$  (Figure 4A). In contrast, TUDCA abrogated nuclear condensation and fragmentation ( $P < 0.01$ ). Similar results were obtained in caspase-3 activity assays ( $P < 0.05$ ) (Figure 4B).

Next, we investigated if A $\beta_{1-42}$ -induced caspase activation was responsible for cleavage of tau. Immunofluorescence assays showed that nuclear fragmentation and active caspase-3 often were colocalized with Asp421-cleaved tau in cortical neurons undergoing apoptosis (Figure 5A). Interestingly, cleaved tau was distributed abnormally within the neurons and detected in cell bodies. In addition, immunoblotting revealed that cleaved tau was upregulated by almost ten-fold after incubation with A $\beta_{1-42}$  ( $P < 0.05$ ) (Figure 5B). Notably, TUDCA reduced caspase-cleaved tau to control values ( $P < 0.05$ ); and this was further confirmed by immunofluorescence. Similar results were obtained using the pan caspase inhibitor Z-VAD-FMK (data not shown). These results showed that fibrillar A $\beta_{1-42}$  decreased cell viability, and induced apoptosis with subsequent cleavage of tau, which may precede tau aggregation in NFT.

**DISCUSSION**

The precise molecular mechanisms involved in AD-related neuronal death and

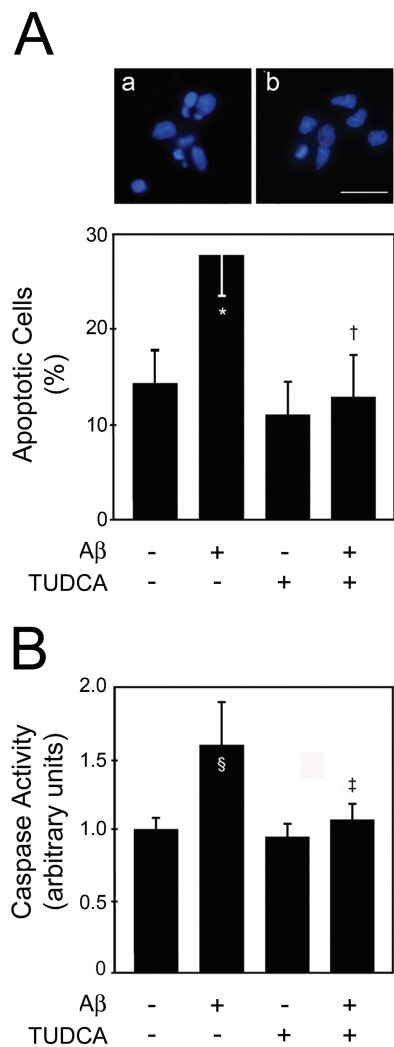


**Figure 4.** TUDCA inhibits apoptosis and caspase-3 activation in primary cortical neurons incubated with fibrillar A $\beta_{1-42}$ . Cells were incubated with 20  $\mu$ M fibrillar A $\beta_{1-42}$ , or no addition (control),  $\pm$  100  $\mu$ M TUDCA for 24 h. In coinubation experiments, TUDCA was added 12 h prior to incubation with A $\beta_{1-42}$ . Cells were fixed and stained for microscopy assessment of apoptosis. Cytosolic proteins were extracted for caspase-3-like activity assays. A: Fluorescence microscopy of Hoechst staining in controls (a); and in cells exposed to A $\beta_{1-42}$  (b) (top) and percentage of apoptosis (bottom). Apoptotic nuclei were identified by condensed chromatin as well as nuclear fragmentation. B): DEVD-specific caspase activity. The results are expressed as mean  $\pm$  SEM of at least three different experiments. \* $P < 0.01$  and § $P < 0.05$  from control; † $P < 0.01$  and ‡ $P < 0.05$  from A $\beta$ . Scale bar: 15  $\mu$ m.

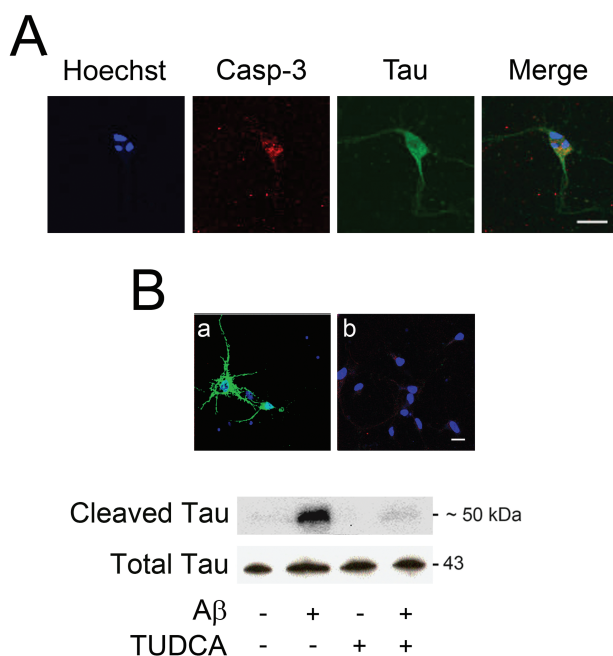


**Figure 5.** TUDCA modulates cleavage of tau by caspase-3 in primary cortical neurons incubated with fibrillar  $A\beta_{1-42}$ . Cells were incubated with 20  $\mu$ M fibrillar  $A\beta_{1-42}$ , or no addition (control),  $\pm$  100  $\mu$ M TUDCA for 24 h. In coinubation experiments, TUDCA was added 12 h prior to incubation with  $A\beta_{1-42}$ . Colocalization of active caspase-3 and cleaved tau was evaluated by confocal immunofluorescence microscopy. Apoptotic nuclei were visualized with Hoechst staining. Total proteins were extracted and subjected to Western blot analysis. A: Confocal microscopy and colocalization of apoptotic nuclei, active caspase-3, and cleaved tau in cells exposed to  $A\beta_{1-42}$ . B: Confocal microscopy and colocalization of apoptotic nuclei and cleaved tau in cells exposed to  $A\beta$  (a) and  $A\beta$  + TUDCA (b) (top); representative immunoblot of caspase-cleaved tau in cells after treatment with  $A\beta$   $\pm$  TUDCA (bottom). The blot was normalized to total tau protein levels. Scale bar: 20  $\mu$ m.

cognitive decline are not understood entirely. Aggregation of tau into insoluble NFT and formation of extracellular plaques by  $A\beta$  are the most characterized pathological features in AD. Nevertheless, the correlation between these abnormal entities and their role in neuronal death is still unclear. Implication of apoptosis as a general mechanism in many neurodegenerative disorders, including AD, has been supported by several studies (26). In addition, we have reported previously that antiapoptotic treatment with TUDCA prevents  $A\beta$ -induced degeneration in neuronal cells (15–17). In the present study, we provide evidence that apoptosis is an early event in the frontal cortex and hippocampus of rTg4510 mice. Moreover, caspase-3 activation is associated with cleavage of tau

in its C-terminal region, which precedes NFT formation. Cleaved tau represents potentially intermediate neurotoxic species that are correlated with initial neuronal dysfunction. Finally, antiapoptotic TUDCA prevents cleavage of tau from  $A\beta$ -induced apoptosis in cultured neurons, underscoring the role of modulation of apoptosis in tau cleavage.

Previous studies have shown that the rTg4510 mouse is a remarkable model of tauopathy. Tau expression induces age-dependent memory impairment, NFT formation and memory loss (10–12). Transgenic aged mice undergo massive neuronal loss, but the mechanisms by which neurons die are still not clear. In addition, although expressed in all fore-brain structures, the transgene tau with the P301L mutation affects only specific

brain regions. Neuronal loss is > 80% in hippocampal area CA1 and dentate gyrus, and ~50% in cortex by 8.5 months (12). These results are consistent with the regional specificity observed in tauopathies, including AD (24).

Here, we investigated whether apoptosis is involved primarily in neuronal loss of rTg4510 mice. DNA fragmentation and caspase activation were evident in transgenic animals at 2.5 months. In fact, TUNEL-positive cells were easily detected in the frontal cortex, subgranular zone of the dentate gyrus, and subventricular zone. Interestingly, the subgranular zone gives rise to neural stem cells that ultimately differentiate into granule cell neurons. Therefore, apoptosis seen in the subgranular zone may account for the loss of granule cells. Levels of apoptosis were still elevated slightly in the subgranular zone at 5.5 months, but showed no changes at 8.5 months. Activation of caspase-3 was no longer evident at 5.5 and 8.5 months. Interestingly, apoptosis was increased in the medial septal nucleus at all ages, and in the sensorimotor cortex in older animals. We also were unable to detect significant levels of apoptosis in hippocampal CA1 of rTg4510 mice. Thus, caspase-dependent and -independent cell death is confined to specific areas, possibly signaling other brain regions.

Evidence of apoptosis in AD has been supported largely by tissue culture studies (26). Contradictory results came from observations of human post-mortem brain tissue, where clear detection of apoptotic cells is difficult (27). This may be explained by the fact that cell death in AD occurs over decades, while apoptosis is executed within a few hours. Thus, synchronous detection of a substantial number of apoptotic cells at any given time would be very difficult. In addition, there is strong evidence to suggest that apoptotic mechanisms may play an important role in disease pathogenesis, even in the absence of overt apoptosis (28). Our results suggest that apoptosis, rather than being responsible for extensive neuronal loss in older ani-

mals, triggers toxic events that ultimately contribute to cognitive deficits. In fact, activation of caspase-3 in the frontal cortex and hippocampus resulted in cleavage of tau in rTg4510 mice at 2.5 months. Neurons with active caspase-3 often showed Asp421-cleaved tau. Caspase-3 cleavage of tau is thought to induce abnormal conformations by removing part of the C-terminal region, which is essential to inhibit tau aggregation *in vitro* (29,30). Although early apoptosis also may represent a developmental-related phenomenon (11), it is clear that the cleavage of tau is a toxic process with potentially important neurodegenerative repercussions.

Importantly, the formation of NFT appears to be dissociated from neuronal loss in rTg4510 mice. It has been shown that, at 4 months of age, ~50% of neurons in the dentate gyrus were lost before any early conformational changes in tau were detectable (12). In addition, after transgene suppression, neuronal loss was prevented and memory decline reverted, but NFT continued to accumulate (10,12). Interestingly, rT4510 mice developed the first signs of cognitive decline at 2.5 months, coincident with cleavage of tau. Thus, it is possible that deficits in neurons occur in the early stages of disease, resulting from aberrant forms of tau, prior to massive neuronal loss and NFT formation. In this scenario, apoptosis and subsequent cleavage of tau are strong candidates to trigger the primary deleterious effects on neuronal function.

The identification of two forms of tau multimers with 140 and 170 kDa have been described recently in rTg4510 mice (31). The molecular weights suggest an oligomeric aggregate of the soluble and insoluble forms of tau, respectively. The aggregates accumulate early in the pathogenesis and appear to be associated with the development of functional deficits. Thus, it is tempting to speculate that cleavage of tau occurs prior to formation of the first oligomers, thus promoting their aggregation. Further, the fact that cleaved tau was found in older animals suggests that although cleavage

may occur early in NFT formation, the resultant fragment persists throughout NFT evolution. It is possible that apoptosis continues beyond 2.5 months and up to 5.5 months, which explains the accumulation of cleaved tau in older animals (32). On the other hand, calpains might be responsible for cleavage of tau in brain areas where caspase-3 activation was not detected, including the olfactory bulb, sensorimotor cortex, and entorhinal cortex, although further investigation is required. In this scenario, apoptosis may represent the triggering event for the formation and aggregation of intermediate species of tau in frontal cortex and hippocampus, which ultimately result in massive non-apoptotic neuronal death.

The efficacy of the rTg4510 mouse model relies on the capacity of mutated tau to induce neuronal modifications. Mutations of tau reduce its ability to interact with microtubules and are associated with tauopathies (33). These disorders are distinct from AD because there is no evidence for A $\beta$ , APP, or presenilin involvement. In AD, however, A $\beta$  plays an important role in neuronal toxicity and cell death, and its involvement in tau pathology cannot be neglected. Indeed, both mutations of APP with A $\beta$  deposition and intracranial injection of A $\beta$  increased NFT formation in transgenic mice expressing a frontotemporal dementia with parkinsonism linked to chromosome 17-causing mutant (25,34). Several evidences suggest that the link between A $\beta$  and tau is predominantly, if not exclusively, unidirectional. In fact, tau has no effect on the onset and progression of A $\beta$  accumulation (35). Rather, tau accumulation occurs after amyloid plaques formation, further exacerbating the neurotoxicity induced by A $\beta$ . In fact, it has been shown recently that overexpression of tau with the P301L mutation induces mitochondria dysfunction, increasing the production of reactive oxygen species and the vulnerability to A $\beta$  insults (36). Moreover, reduction of endogenous tau levels proved to inhibit behavioral deficits in transgenic expressing human APP, without altering A $\beta$  levels (37).

Recent studies suggest that A $\beta$  accumulation and caspase activation precedes and induces cleavage of tau and NFT formation (7,9). Our results confirmed that fibrillar A $\beta$ <sub>1-42</sub> induces toxicity, nuclear fragmentation, and caspase-3 activation, which was associated with cleavage of tau. Moreover, cleaved tau often was co-localized with active caspase-3 in neurons undergoing nuclear modifications. Thus, apoptotic events and cleavage of tau occur almost simultaneously in neurons exposed to aggregated A $\beta$ .

TUDCA prevented apoptosis and caspase-3 activation after incubations of neurons with fibrillar A $\beta$ <sub>1-42</sub>, thus reducing caspase-cleaved tau. In fact, by modulating neuronal death, TUDCA additionally interferes with subsequent downstream production of toxic mediators of AD-associated pathology. This suggests that TUDCA may inhibit further aggregation of tau in NFT and promote cell survival. It would be interesting to investigate whether administrations of TUDCA to newborn or up to 2.5 months rTg4510 mice would prevent cleavage of tau, and subsequent massive neuronal loss, memory decline, and NFT formation.

Collectively, the present study provides evidence that apoptosis may represent a crucial event in AD and other tauopathies. Either by promoting further cell death or activating toxic effectors, apoptosis interferes with the pathogenesis of the disease. In rTg4510 mice, apoptosis is an early event in the frontal cortex and hippocampus, occurring prior to NFT formation and massive neuronal death. Caspase-3-cleaved intermediate tau species may represent intermediate toxic forms of tau in rTg4510 brains and in A $\beta$ -exposed cultured neurons, although triggered by different mechanisms. The presence of this cleaved form of tau may precede its aggregation in NFT and induce neuronal dysfunction. These results underscore the importance of antiapoptotic agents in treating neurodegeneration associated with AD and other tauopathies.



## ACKNOWLEDGMENTS

We are grateful to Karen H Ashe, University of Minnesota; Minneapolis, Minnesota, United States of America for providing the rTg4510 mice. This work was supported in part by grants POCL/SAU-MMO/57936/2004 and PTDC/SAU-FCF/67912/2006 from Fundação para a Ciência e Tecnologia (FCT), Lisbon, Portugal. R.M.R and R.S.V. were recipients of Ph.D. fellowships (SFRH/BD/12641/2003 and SFRH/BD/30467/2006, respectively), and R.E.C. was recipient of Postdoctoral fellowship (SFRH/BPD/30257/2006) from FCT.

## REFERENCES

- Selkoe DJ. (2001) Alzheimer's disease: genes, proteins, and therapy. *Physiol. Rev.* 81:741–66.
- Mandelkew EM, Mandelkew E. (1998) Tau in Alzheimer's disease. *Trends Cell. Biol.* 8:425–7.
- Alonso A, Zaidi T, Novak M, Grundke-Iqbal I, Iqbal K. (2001) Hyperphosphorylation induces self-assembly of tau into tangles of paired helical filaments/straight filaments. *Proc. Natl. Acad. Sci. U. S. A.* 98:6923–8.
- Gamblin TC, Berry RW, Binder LI. (2003) Tau polymerization: role of the amino terminus. *Biochemistry.* 42:2252–7.
- Su JH, Anderson AJ, Cummings BJ, Cotman CW. (1994) Immunohistochemical evidence for apoptosis in Alzheimer's disease. *Neuroreport.* 5:2529–33.
- Selznick LA *et al.* (1999) *In situ* immunodetection of neuronal caspase-3 activation in Alzheimer disease. *J. Neuropathol. Exp. Neurol.* 58:1020–6.
- Rissman RA *et al.* (2004) Caspase-cleavage of tau is an early event in Alzheimer disease tangle pathology. *J. Clin. Invest.* 114:121–30.
- Newman J *et al.* (2005) Caspase-cleaved tau accumulation in neurodegenerative diseases associated with tau and alpha-synuclein pathology. *Acta Neuropathol. (Berl.)* 110:135–44.
- Gamblin TC *et al.* (2003) Caspase cleavage of tau: linking amyloid and neurofibrillary tangles in Alzheimer's disease. *Proc. Natl. Acad. Sci. U. S. A.* 100:10032–7.
- Santacruz K *et al.* (2005) Tau suppression in a neurodegenerative mouse model improves memory function. *Science.* 309:476–81.
- Ramsden M *et al.* (2005) Age-dependent neurofibrillary tangle formation, neuron loss, and memory impairment in a mouse model of human tauopathy (P301L). *J. Neurosci.* 25:10637–47.
- Spires TL *et al.* (2006) Region-specific dissociation of neuronal loss and neurofibrillary pathology in a mouse model of tauopathy. *Am. J. Pathol.* 168:1598–607.
- Rodrigues CMP *et al.* (2000) Tauroursodeoxycholic acid partially prevents apoptosis induced by 3-nitropropionic acid: evidence for a mitochondrial pathway independent of the permeability transition. *J. Neurochem.* 75:2368–79.
- Rodrigues CMP, Fan G, Ma X, Kren BT, Steer CJ. (1998) A novel role for ursodeoxycholic acid in inhibiting apoptosis by modulating mitochondrial membrane perturbation. *J. Clin. Invest.* 101:2790–9.
- Solá S, Castro RE, Laires PA, Steer CJ, Rodrigues CMP. (2003) Tauroursodeoxycholic acid prevents amyloid-beta peptide-induced neuronal death via a phosphatidylinositol 3-kinase-dependent signaling pathway. *Mol. Med.* 9:226–34.
- Ramalho RM *et al.* (2006) Tauroursodeoxycholic acid modulates p53-mediated apoptosis in Alzheimer's disease mutant neuroblastoma cells. *J. Neurochem.* 98:1610–8.
- Ramalho RM *et al.* (2004) Inhibition of the E2F-1/p53/Bax pathway by tauroursodeoxycholic acid in amyloid beta-peptide-induced apoptosis of PC12 cells. *J. Neurochem.* 90:567–75.
- Keene CD *et al.* (2002) Tauroursodeoxycholic acid, a bile acid, is neuroprotective in a transgenic animal model of Huntington's disease. *Proc. Natl. Acad. Sci. U. S. A.* 99:10671–6.
- Rodrigues CMP *et al.* (2002) Neuroprotection by a bile acid in an acute stroke model in the rat. *J. Cereb. Blood Flow Metab.* 22:463–71.
- Rodrigues CMP *et al.* (2003) Tauroursodeoxycholic acid reduces apoptosis and protects against neurological injury after acute hemorrhagic stroke in rats. *Proc. Natl. Acad. Sci. U. S. A.* 100:6087–92.
- Duan WM, Rodrigues CMP, Zhao LR, Steer CJ, Low WC. (2002) Tauroursodeoxycholic acid improves the survival and function of nigral transplants in a rat model of Parkinson's disease. *Cell Transplant.* 11:195–205.
- Ved R *et al.* (2005) Similar patterns of mitochondrial vulnerability and rescue induced by genetic modification of alpha-synuclein, parkin, and DJ-1 in *Caenorhabditis elegans*. *J. Biol. Chem.* 280:42655–68.
- Brewer GJ, Torricelli JR, Evege EK, Price PJ. (1993) Optimized survival of hippocampal neurons in B27-supplemented Neurobasal, a new serum-free medium combination. *J. Neurosci. Res.* 35:567–76.
- Braak H, Braak E. (1991) Neuropathological staging of Alzheimer-related changes. *Acta Neuropathol. (Berl.)* 82:239–59.
- Gotz J, Chen F, van Dorpe J, Nitsch RM. (2001) Formation of neurofibrillary tangles in P301L tau transgenic mice induced by Abeta 42 fibrils. *Science.* 293:1491–5.
- Fadeel B, Orrenius S. (2005) Apoptosis: a basic biological phenomenon with wide-ranging implications in human disease. *J. Intern. Med.* 258:479–517.
- Migheli A, Cavalla P, Marino S, Schiffer D. (1994) A study of apoptosis in normal and pathologic nervous tissue after *in situ* end-labeling of DNA strand breaks. *J. Neuropathol. Exp. Neurol.* 53:606–16.
- Dickson DW. (2004) Apoptotic mechanisms in Alzheimer neurofibrillary degeneration: cause or effect? *J. Clin. Invest.* 114:23–7.
- Abraha A *et al.* (2000) C-terminal inhibition of tau assembly *in vitro* and in Alzheimer's disease. *J. Cell. Sci.* 113 Pt 21:3737–45.
- Berry RW *et al.* (2003) Inhibition of tau polymerization by its carboxy-terminal caspase cleavage fragment. *Biochemistry.* 42:8325–31.
- Berger Z *et al.* (2007) Accumulation of pathological tau species and memory loss in a conditional model of tauopathy. *J. Neurosci.* 27:3650–62.
- Park SY, Ferreira A. (2005) The generation of a 17 kDa neurotoxic fragment: an alternative mechanism by which tau mediates beta-amyloid-induced neurodegeneration. *J. Neurosci.* 25:5365–75.
- Goedert M, Crowther RA, Spillantini MG. (1998) Tau mutations cause frontotemporal dementias. *Neuron.* 21:955–8.
- Lewis J *et al.* (2001) Enhanced neurofibrillary degeneration in transgenic mice expressing mutant tau and APP. *Science.* 293:1487–91.
- Oddo S *et al.* (2007) Genetically augmenting tau levels does not modulate the onset or progression of Abeta pathology in transgenic mice. *J. Neurochem.* 94:1711–8.
- David DC *et al.* (2005) Proteomic and functional analyses reveal a mitochondrial dysfunction in P301L tau transgenic mice. *J. Biol. Chem.* 280:23802–14.
- Roberson ED *et al.* (2007) Reducing endogenous tau ameliorates amyloid beta-induced deficits in an Alzheimer's disease mouse model. *Science.* 316:750–4.